

Usual and unusual crystallization from solution

Eve Revalor^a, Zoubida Hammadi^a, Jean-Pierre Astier^a, Romain Grossier^a, Eric Garcia^b, Christian Hoff^b, Kenji Furuta^c, Tetsuo Okustu^c, Roger Morin^a, Stéphane Veesler^{a,*}

^a Centre Interdisciplinaire de Nanosciences de Marseille, CNRS, Aix-Marseille Université, CINAM-UPR3118, Campus de Luminy, Case 913, 13288 Marseille Cedex, France

^b Sanofi-Aventis Chimie, Route d'Aramon, 30390 Aramon, France

^c Gunma University, Kiryu 375-8515, Japan

ARTICLE INFO

Article history:

Received 26 October 2009

Accepted 3 January 2010

Communicated by J. de Yoreo

Available online 11 January 2010

Keywords:

A1. Nucleation

A2. External fields

A2. Growth from solutions

ABSTRACT

Nucleation is a stochastic phenomenon and the probability of observing the critical nuclei formation is very low. Our aim is to enhance nucleation in the metastable zone enabling us to locate and control it.

The first step is to determine the nucleation rate, and thus the nucleation behavior of the molecule studied. The two usual methods for determining nucleation rate are measuring induction time by direct counting/observation and direct determination of the steady-state rate of homogeneous nucleation.

The second step consists in acting on nucleation, to control, locate and observe it. We develop unusual approaches, adding an external field to the crystallization conditions or using confinement. Ultrasounds reduce induction time and increase the number of crystals. The light irradiation induces nucleation by forming radicals. The electric field tends to localize the nucleation near one electrode depending on the polarity of the molecule studied in acting locally on the density of the solution. Lastly confinement was tested, and results indicate that this approach is very promising for controlling nucleation spatially and generate one single crystal per droplet.

© 2010 Elsevier B.V. All rights reserved.

1. Introduction

The study of the impact of crystallization on crystal properties is one of the most important areas of industrial crystallization. By crystal properties we intend crystal habit, crystal size distribution and phases. Although a great deal is known about crystal growth, considerably less is known about crystal nucleation because of the difficulty of directly observing the nuclei. Questions remain about the structure and size of nucleating crystallites. The reason for this is that since nucleation is a stochastic phenomenon, the probability of observing the first nuclei is very low, for spatial and temporal reasons. Here, our aim is to enhance nucleation in the metastable zone enabling us to locate and control it.

Our paper presents perspectives in the field of nucleation studies. The paper begins with a bibliographical analysis of nucleation rate measurements and the use of an external field (electric and magnetic field, ultrasound and light irradiation) and of confinement. Then, we present different experimental unusual approaches to control and locate the nucleation.

2. Bibliographical studies and experimental section

2.1. Determination of nucleation rate

Many studies have shown different ways to determinate nucleation rate. All agree on one point: extensive work and large quantities of raw material are required. Because nucleation is a stochastic phenomenon, a lot of experiments under identical conditions are needed. For each set of conditions, at least a hundred of experiments are required, so that a statistical law can be applied.

Studies on the nucleation theory started decades ago. There are essential references such as Zettlemoyer [1] on nucleation from a theoretical point of view, presenting kinetics and thermodynamics equations. Boistelle and Astier [2], however, concentrated on finding the kinetics and thermodynamics equations of nucleation in solution (Eq. 1).

$$J = K_0 \exp(-\Delta G^*/k_B T) \quad (1)$$

With J the nucleation rate in number $s^{-1} m^{-3}$, K_0 the kinetic factor ($m^{-3} s^{-1}$), ΔG^* the activation free energy (J), k_B the Boltzmann constant ($J K^{-1}$) and T the temperature (K).

In practice, the two usual methods of nucleation-rate determination are measuring the induction time by direct counting/observation and direct determination of the steady-state rate of homogeneous nucleation.

* Corresponding author. Tel.: +336 6292 2866; fax : +334 9141 8916.
E-mail address: veesler@cinam.univ-mrs.fr (S. Veesler).

The first method consists in establishing supersaturation, and then measuring the time that crystals take to become observable, namely the induction time. This method was detailed by Boistelle and Astier [2]: plotting the inverse of induction time as a function of the square logarithm of supersaturation gives the interfacial energy (γ) and the kinetic factor K_0 . Actually, the supersaturation range over which the experiment can be performed is rather limited due to the metastable zone. When β is too small heterogeneous nucleation may replace homogeneous nucleation. When β is too large, induction times are difficult to measure because they are too short. In practice, we are able to measure the induction time when it is comprised between 1 s and a few days (around β^* in Fig. 1), that is to say in the vicinity of the metastable zone limit. However, despite these drawbacks, the method provides fairly good values from K_0 and γ .

The second method was proposed by Tsekova et al. [3] who developed a novel technique that allows direct determination of the steady-state rate of homogeneous nucleation. At the beginning of a run, the solution is loaded at a temperature chosen to prevent nucleation of crystals. Then temperature is lowered (respectively raised if the solubility is reversed with T) to a selected T_1 at which nucleation occurs. After a period of Δt_1 temperature is raised (respectively lowered if the solubility is reversed with T) from the nucleation temperature T_1 to the growth temperature T_2 . At T_2 , supersaturation is at a level where nucleation rate is practically zero, but the crystals already formed can grow to detectable dimensions (Fig. 2). This allows separation

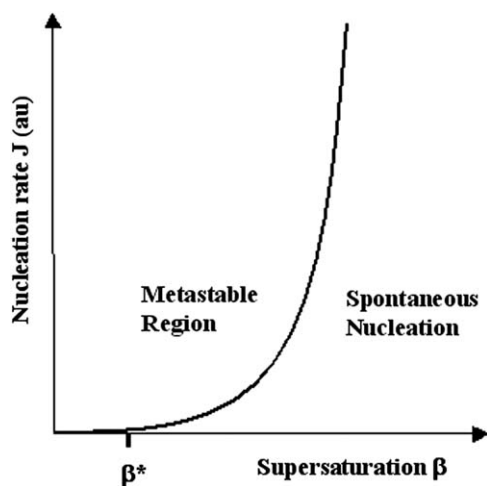


Fig. 1. Nucleation rate J (arbitrary units) versus supersaturation. Below the critical value β^* the solution remains metastable, whereas above β^* the nucleation rate increases drastically.

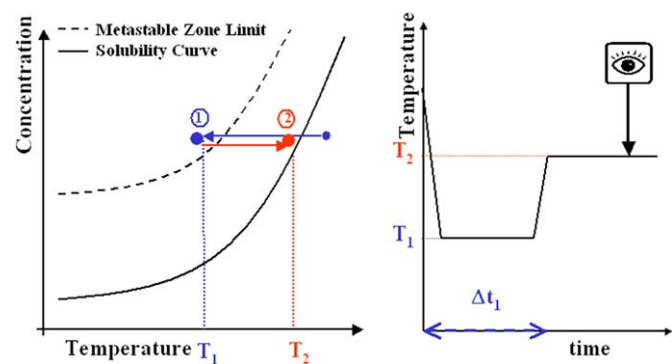


Fig. 2. Principle of the double pulse technique: position in the phase diagram and temperature profile during a nucleation experiment.

between the nucleation and the ensuing growth. After the growth stage, the crystals nucleated at T_1 during Δt_1 are counted. After plotting the number of crystals nucleated as a function of Δt_1 , the steady state nucleation rate can be determined as represented by the slope of the straight line.

This last method also has limits, Dixit et al. [4] compare it to other methods of determination, and show that this method underestimates the number of crystals nucleated. Indeed, the critical size varies with temperature, so when temperature changes, critical size also changes: at the nucleation temperature, the critical size is smaller than that at the growth temperature. Therefore, while the temperature is rising up to the growth temperature, nuclei bigger than the critical size at the nucleation temperature, but smaller than that at the growth temperature, are dissolved. Consequently, at the end of experiments, fewer crystals have been grown than were nucleated at the beginning. But this needs to be discussed for each experimental case; for example in the case of a system having a solubility, which increases when T decreases, growth temperature (T_2) is higher than nucleation temperature (T_1) as it is the case for BPTI (see Section 3.1).

2.2. Unusual crystallization

2.2.1. External fields

The implications of an external field for crystal growth in solution were highlighted by Voss [5] and Oxtoby [6]. Two effects on the structure of the supersaturated solutions are expected: molecular orientation and density fluctuation. We are interested in phenomena produced by external fields that have an influence on nucleation. In the following, we present a short bibliographic study on the effects of different external fields on crystallization and lastly, we present our first experimental results using DC electric internal field, light and ultrasounds irradiation.

The best documented effect is light-induced nucleation. Two cases have been discussed in the literature: first, the non-photochemical light-induced nucleation (NPLIN) using laser and second, photochemical light-induced nucleation (PLIN) using white lights (Xenon lamp).

Non-photochemical light-induced nucleation uses a laser to irradiate the solution. The first to observe an influence of the laser on nucleation was Tam et al. [7]. They worked on vapors of Cesium with small amounts of hydrogen, and observed that upon irradiation by a laser, some particles appeared, which he identified as cesium-hydride crystals. More recently, Garetz et al. [8] worked on supersaturated aqueous urea solutions, and suggested an electric field-induced alignment of the molecules, the optical Kerr effect. Moreover, Zaccaro et al. [9] experiments on glycine lead to different polymorphs depending on whether they are exposed to intense pulses of laser or not. Actually, light-induced nucleated crystals are γ -polymorphs and the control solutions give the α -form. Garetz has even observed that if solutions are irradiated with circular polarization the α -form is formed, but with linear polarization in the irradiation, the γ -polymorph is formed. Oxtoby [6] tries to find reasons for this alignment of molecules, because as Garetz said, if the influence is on the 'prefactor' of the energy barrier, the impact is not great enough to explain the effects. This leaves a challenge for theorists, to discover how laser acts on glycine nucleation.

Okutsu et al. [10] also find an effect of laser on nucleation of benzophenone in ethanol/water mixed solutions, but in this case it is related to photochemistry. Benzophenone is light-sensitive, and when the solution is irradiated, there is less benzopinacol so the benzophenone can crystallize before benzopinacol precipitation. These experiments lead us to the second form of light-induced nucleation, which is photochemical. Okutsu et al. [11], in

experiments on lysozyme solutions irradiated by a Xenon lamp, discovered that irradiation enhanced nucleation, but also observed that there is a irradiation time beyond which the protein is denatured. Veessler et al. [12] proposed seeding non-irradiated solutions of lysozyme with limited amounts of irradiated lysozyme solution, in order to avoid denaturation of protein by excessive irradiation. Moreover, it was demonstrated by absorption experiments that the irradiation of lysozyme [12] and thaumatin [13] produces photochemical intermediate (radicals), which enhances nucleation.

Surprisingly, it is only recently that the effects on crystallization in solution (apart from electrocrystallization) of electric field, have been studied, apart from a theoretical consideration of Kashchiev [14] and an experimental paper of Chin et al. [15] coupling zone electrophoresis to membrane dialysis. For instance, Taleb et al. [16] studied the nucleation rate of protein solution drops placed between two flat electrodes outside the crystallizer. They observed an expansion of the drops until they touch the cathode and then expand to the anode. Then crystallization occurs near the cathode, with fewer but larger crystals under the electric field. In a second study, Taleb et al. [17] observed an improvement in the crystal quality of the crystals nucleated and grown in an electric field.

Nanev and Penkova [18], using the same set-up as Taleb, studied the impact of the electric field as a function of temperature and why nucleation occurs at the cathode. They concluded that the electric field has a bigger impact on nucleation rate and induction time when temperature is lower. Moreover, they observed that, at low temperatures, an electric field increases the number of crystals nucleated.

Mirkin et al. [19] and Moreno and Sasaki [20] developed a set-up for internal application of an electric field on lysozyme solutions, observing a decrease in induction time and in number of crystals in agreement with Taleb's observation. Moreover, Moreno and Sasaki [21] observe an amorphous phase forming around the cathode, also observed by Nanev and Penkova [18] and Penkova et al. [22] with solutions of ferritin and apoferritin. They observed that in drops, the number of crystals nucleated under electric field decreased, while when the electric field is applied to a vessel, the number of crystals is increased.

The third electromagnetic field, the magnetic field, has been studied for at least 40 years. According to Worcester [23], many protein structures exhibit diamagnetic anisotropy resulting from the contribution of the planar peptide bonds of the molecules and aromatic amino-acid residues. For α -helices, these bond planes are oriented parallel to the helix axis which is, therefore, of lesser diamagnetic susceptibility. This explains why proteins and synthetic polypeptides exhibit magnetic orientation with the α -helices parallel to the magnetic field. In the literature, most studies focus on the magnetic birefringence (Cotton–Mouton effect) of aromatic or aliphatic compounds [24] or biological systems [25–27].

Diamagnetic anisotropy is identified either by direct observation of the formation of oriented fibrin, of small crystals or by the anisotropy of a scattering pattern. It is only recently, that protein crystals have been nucleated and grown in the presence of a magnetic field [28–31]. Moreover, crystal growth of benzophenone under high magnetic fields was reported recently [32]. A rapid calculation [29] shows that under a field of 1.25 T, 10^7 lysozyme molecules are required to counteract the thermal energy, indicating that individual molecules are not oriented in solution. Magnetic field has an effect on crystal orientation but not on nucleation.

Lastly, ultrasounds is a promising external field for crystal nucleation by nucleating in the metastable zone. It has been studied for decades. Hem [33], in 1967, researched the effects of

ultrasounds on nucleation explaining that the cavitation bubbles, in inducing drastic conditions in their vicinity, are the key of the mechanism: pressure of the collapse of the cavitation bubble, high cooling rate effect and/or heterogeneous nucleation on the bubble interface are the most common hypothesis. This last hypothesis, heterogeneous nucleation, tends to be abandoned. Concerning the high pressure hypothesis, several studies tried to modelize it [34–36], but there are still large discrepancies with experiments. For the cooling rate hypothesis, care must be taken because of the relative thickness of the thermal diffusion layer around the bubble, and its quite low temporal existence. [37,38] Nevertheless, these hypotheses are still under debate. Lastly, another hypothesis was proposed by Louisnard et al. [39], arguing the accelerations present at the bubble collapse ($10^{12}g$) could segregate species in the vicinity of the bubble, and a mechanism explaining impact on nucleation rate has been proposed [40].

In practice, Lyczko et al. [41], investigated the effect of ultrasounds on induction time and metastable zone width. They observed that ultrasounds reduced induction time of crystal nucleation of potassium sulfate. Moreover, induction time depends on the power of ultrasounds, the higher the power, the lower the induction time. Guo et al. [42] observed the same phenomenon on barium sulphate homogeneous nucleation, and postulated that the ultrasounds increased the diffusion coefficient, this acceleration being the main reason for reduce induction time. Ueno et al. [43] worked on the crystallization of fats, like tripalmitin (PPP) and trilaurin (LLL). They also observed that ultrasounds decrease induction time, and furthermore, that without ultrasounds, tripalmitin and trilaurin crystallized under two polymorphic phases, while with the application of ultrasounds, only one crystallizes. Nanev and Penkova [44] observed an increase in the number of crystals nucleated.

2.2.2. Confinement

The effect of confinement on nucleation was recently theoretically reconsidered and a clear window of parameters, where a single nuclei occurs alone, was identified [45]. Confinement where experimentally affordable, will provide a new way to study critical clusters and nucleation. In the literature confinement, at the nanometer scale, is realized by controlled-pore glasses [46,47] or other nanoporous materials [48]. Thermal behavior of materials under confinement is examined in relation with the Gibbs–Thomson equation [47], or polymorph selectivity in ultra-small pores [48,49] or in small droplets [50]. Microemulsions are also used to produce confinement in order to measure critical nucleus size via thermal behavior [51]. Droplet generation is a very promising approach because it allows direct observation under optical microscope. We have developed a set-up to generate and observe micrometer droplets of sodium chloride solutions [52].

3. Experimental part

3.1. Determination of nucleation rate

BPTI (bovine pancreatic trypsin inhibitor) (6511 Da, $pI=10.5$), was supplied as a lyophilized powder by Bayer and used as received. BPTI is employed to reduce blood loss during complex surgery. Proper amounts of BPTI and NaCl were dissolved in pure water (ELGA UHQ reverse osmosis system) to obtain stock solutions needed for crystallization experiments. The different solutions were buffered with 80 mM acetic acid, adjusted to $pH=4.5$ with NaOH (4 M) and filtered through 0.22 μm Millipore filters. BPTI concentrations were controlled by optical density

measurements (Kontron UVKON810) using an extinction coefficient of $0.786 \text{ cm}^{-1} \text{ mL mg}^{-1}$ at 280 nm [53].

The first experiments were performed in Microbatch[®], with some inert paraffin oil (HR3-42) above all the batch, in order to avoid evaporation. We prepared solutions with different concentrations, between the solubility and the metastable zone limit. Then we measured the time that crystals took to be observable.

Secondly we use the method described by Tsekova et al. [3]. We prepared 2 mL of solution of BPTI and we distribute 20 μL of it in 96 cells of 100 μL . 10 μL of inert paraffin oil was then added to each cell on the top of the solutions. The 96 cells are inserted into two blocks thermostated independently by Peltier effect and observed by a microscope (Nikon Diaphot). The whole assembly is mounted on a X–Y translation stage. Sequential image acquisitions performed automatically every hour. At the end of the experiment crystals are counted. The multiwell set-up (ANACRISMAT, France) used here was previously described [54].

3.2. Electric field

BPTI was used at a concentration of 20 mg mL^{-1} , in acetate buffer at 80 mM, pH=4.5 and 1.6 M of NaCl. All the experiments were performed at 20 °C.

In our experimental set-up [55], we use internal electric field, with very weak current, less than 1 μA . All experiments were performed in a glass vessel inserted in a thermostated cell under an optical microscope (Nikon Diaphot).

We made the electrode from W wires (125 μm diameter) consisting of a sharp metallic tip emerging from the end of a glass capillary. First, a tungsten polycrystalline wire is placed inside a glass tube, internal and external diameters of the tube are 300 μm and 1 mm, respectively. Secondly, electrical connections are made to the electrodes. Finally, the tip is fabricated by electrolytic etching in a 2 M NaOH solution [56].

One of the electrodes was sharp and the other was rounded. The distance between the electrodes was roughly 600 μm . The electrodes were placed near the bottom of the crystallization cell. 500 μL of a supersaturated but metastable protein solution was placed in a 10 mm diameter glass vessel; an upper layer of 300 μL of inert paraffin oil (HR3-42) was added to avoid evaporation during the experiments. In all the experiments, direct voltage was applied to the electrodes. It is noteworthy that all the experimental solutions of this study are in the metastable zone for nucleation under normal conditions that is without an external energy field.

3.3. Light irradiation

We used a xenon lamp for light irradiation experiments of BPTI solutions. We therefore carried out nucleation experiments using a “liquid-seeding” technique. The principle of the experiment is as follows: 1.5 mL of a 4 mg mL^{-1} BPTI solution containing 3.2 M NaCl in a 80 mM NaAc buffer solution at pH 4.5 placed in a 0.2 cm \times 1 cm \times 4 cm optical cell hermetically closed to prevent evaporation was irradiated for different times by light from an Xe lamp. 3 μL of the irradiated solution, namely, the liquid seed, was mixed with 3 μL of three concentrated BPTI solutions, 36, 28 and 20 mg mL^{-1} in a 80 mM NaAc buffer at pH 4.5 and placed in a microbatch plate kept at 20 °C to avoid nucleation during the growth process. Thus, the final solutions were 20, 16 and 12 mg mL^{-1} BPTI and 1.6 M NaCl at pH 4.5 in a buffer solution at a final supersaturation of 2, 1.6 and 1.2. In addition, a control solution was prepared with a non-irradiated BPTI solution. Finally, to avoid undesired heterogeneous nucleation due to evaporation from the vapor–solution interface of the droplets, we

used an inert paraffin oil (HR3-42) to cover the droplets. The solution was pipetted through the oil. We observed the plate with a microscope.

3.4. Ultrasounds

The (*R*) (*N*)-[1-[3-[1-benzoyl-3-(3,4-dichlorophenyl) piperidin-3-yl] propyl]-4-phenylpiperidin-4-yl]-*N*-methylacetamide (named API, $M_w=606.6 \text{ g mol}^{-1}$) was provided as a solid by Sanofi-Aventis. It is used as an antagonist of the Neurokinin receptors (NK3) to cure schizophrenia. It was dissolved in 60% of pure ethanol and 40% of pure water as required by the crystallization process.

All experiments were performed in glass vessels capped, usually used for chromatography (0.8 mL vials from RESTEK).

Solutions of different metastable supersaturations were exposed to the ultrasounds by a sonicator (Suprasson Piezo Endo of Satelec 0.1 W) with a sharp tip, during different times, before the vessels were capped. Then the experiments were thermostated and observed under a microscope (Nikon Diaphot).

3.5. Confinement

Experiments consist in crystallizing NaCl by evaporation of micrometer droplets of undersaturated 0.7 M NaCl solutions covered by DMS oil. All experiments were performed on a 18 mm diameter coverslip inserted in a thermostated well under an optical microscope (Zeiss Axio Observer D1). The well is filled with inert DMS oil (Hampton Research HR3-419). The micrometer droplets of NaCl solution are generated on the coverslip by a microinjector (Femtojet, Eppendorf). A home-made micromanipulator consisting of 3 miniature translation stages (piezo electric, MS30 mechanics) allows displacement of the injector (capillary holder) in X, Y and Z with a displacement of 18 mm in the 3 directions by steps of 16 nm. A hydrophobic glass capillary, obtained by vapor-depositing toluene +5%v/v n-octadecyltrichlorosilane (ODTS) mixture on the capillary, with an internal diameter of 0.5 μm (Femtotip Eppendorf), is used.

4. Results and discussion

4.1. Determination of the nucleation rate

For the first experiments performed in Microbatch[®], we prepared 24 solutions of BPTI from 10 to 56 mg mL^{-1} with an incremental increase in 2 mg mL^{-1} . We put 6 μL of each solution into 3 wells of the Microbatch[®] and then when the paraffin oil covered all the batches, we added 4 μL of a solution of 4 M of NaCl we observed the nucleation ensuing, but the results were not conclusive.

We, therefore, decided to use the Tsekova technique. We prepared a solution of 20 mg mL^{-1} of BPTI in Acetate buffer 80 mM, pH=4.5, NaCl 1.6 M. We filled each cell with 20 μL of the solution, and we put an upper layer of paraffin oil on each solution. To avoid nucleation before the start of the experiments the solutions were prepared at 5 °C (because of the retrograde solubility of BPTI in NaCl solutions). We put the 2 blocks into the multiwell set-up, and we set the temperature at 25 °C, near the metastable zone limit, during a defined time and then return to a temperature near the solubility in the metastable zone, 15 °C, to avoid nucleation during growth time. The crystals were counted after several hours, between 12 and 48 h, at the growth temperature. But the crystal number distribution was too wide to be exploited quantitatively in order to plot the number of

crystals versus the nucleation time, because of the heterogeneous nucleation at the interface between the solution and the inert paraffin oil. But, it was possible to estimate the metastable zone width according to this experiment, at 20 °C in this experimental condition no nucleation was observed for 24 h. In the future we propose to use a microfluidics set-up to determine nucleation frequency and avoid heterogeneous nucleation [57].

4.2. External fields

4.2.1. Electric field

We worked at 20 mg mL⁻¹ of BPTI in acetate buffer at 80 mM, pH=4.5 and NaCl 1.6 M, corresponding to a solution in the metastable zone (see Section 4.1). In this study all the experiments were conducted with a direct voltage and we observed a decrease in nucleation time, an increase in growth kinetics and

often a pre-determined positioning of the crystals. As previously shown by Nieto-Mendoza et al. [58] and by our pH monitoring during some experiments, pH did not change enough to affect solubility. In the literature the directed crystallization of proteins in an electric field is attributed to electromigration. In addition, bubbles are formed due to water electrolysis at voltage values higher than 1 V. For this reason we applied a constant direct voltage of 0.7–0.9 V producing a current around 1 μA depending on the tip geometry and not on the distance between the electrodes. For a voltage of 0.7 V we observed a current of 1 μA, decreasing to 0.6 μA. During the experimental time (12–36 h) no

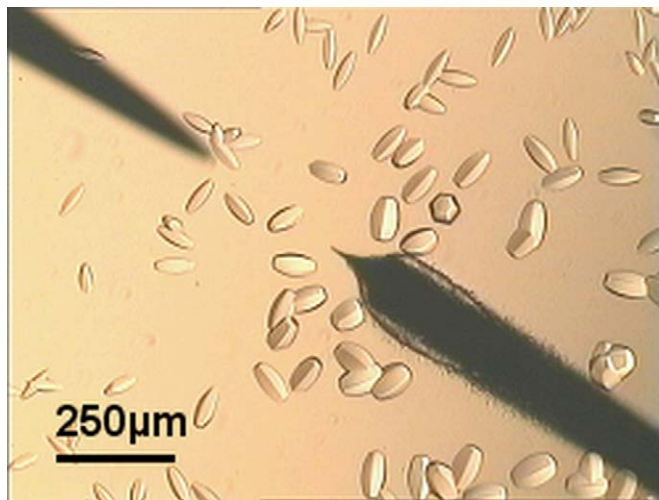


Fig. 3. In situ observations under optical microscopy of BPTI crystallization at 20 °C with a direct voltage of 0.7 V at $t=24$ h (+ indicates the anode).

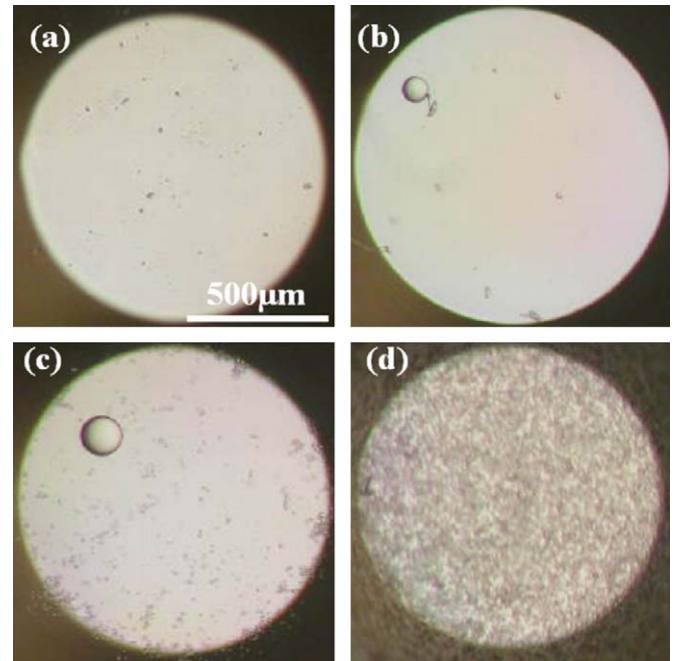


Fig. 5. Photograph of BPTI droplets, 16 mg mL⁻¹, NaAc 80 mM, pH=4.5, irradiation time: 0 min (a), 1 min (b), 3 min (c), 5 min (d).

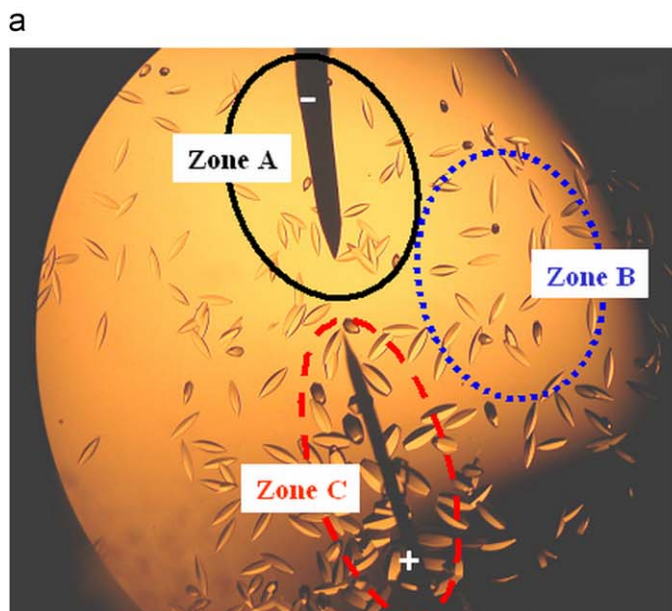
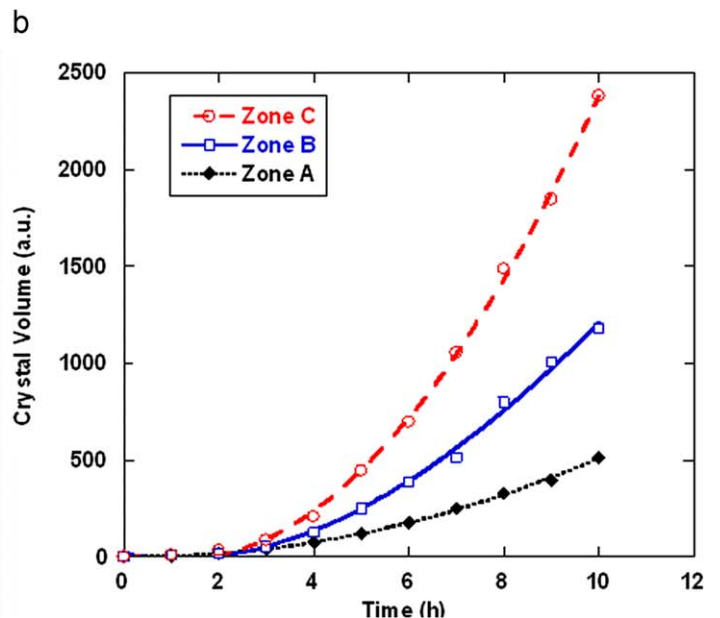


Fig. 4. (a) In situ observations under optical microscopy of BPTI crystallization at 20 °C with a direct voltage of 0.6 V at $t=24$ h (+ indicates the anode) and (b) crystal volume versus time in 3 different zones of the crystallizer.



bubbles were observed. Note that reproducibility was ensured by working at constant initial current.

We observed that the crystals preferentially nucleate at the anode within 1 h, they grow larger near the anode and that a layer is formed around the anode (Fig. 3), identified as a protein-rich phase due to demixion. Moreover, we are able to affirm that there is a concentration gradient due to the electric field from the anode to the cathode, because of the protein-rich phase at the anode,

and that crystals are growing faster near the anode than near the cathode (Fig. 4). Lastly, this is confirmed by the fact that the layer starts to dissolve as soon as polarity is inverted.

4.2.2. Light irradiation

At the end of irradiation, after liquid seeding, we obtain solutions of 12, 16 and 20 mg mL⁻¹, irradiated during 0, 1, 3 and 5 min. In the control solution no crystal was observed in any of the droplets, confirming that the solution was metastable and that undesired heterogeneous nucleation at solution–oil interface or solution–wall-of-the-vessel interface was completely eliminated. In the droplets mixed with irradiated solution, BPTI crystals appeared in the droplets at 16 and 20 mg mL⁻¹ (Fig. 5). Moreover for the solutions at 16 and 20 mg mL⁻¹, there were more crystals as irradiation time increased. These results show unambiguously that light induces nucleation of BPTI.

4.2.3. Ultrasounds

At the end of irradiation with ultrasounds, the solutions contained some crystals. The control solution presented no crystal, but the irradiated cells showed an increase in the number of nucleated crystals and a decrease in the induction time with an increase in the irradiation time (Fig. 6). For small irradiation times, we confirm that ultrasounds induce nucleation in the metastable zone (Fig. 6b and c), in acting on primary nucleation. But in the case of longer irradiation times, secondary nucleation enters in action: already formed crystals are broken and seed the solution (Fig. 6d).

4.2.4. Confinement

Fig. 7 presents the complete process: evaporation, nucleation and growth. After being generated, droplets slowly evaporate until supersaturation is established (Fig. 7a–c). At $t=0$ droplets appear clearer than the oil, because the droplet refractive index of

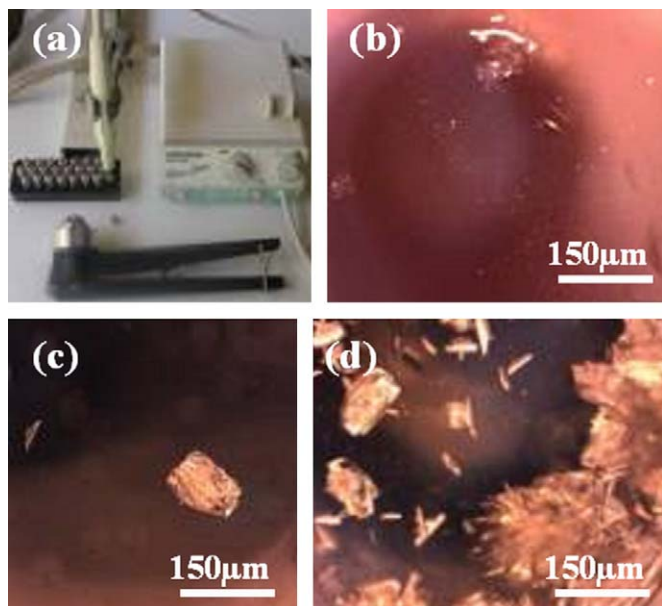


Fig. 6. Experimental set-up (a). Solutions of API ($\beta=3.5$) irradiated by the sonicator at 0.1 W during 0 min (a), 1 min (b) and 2 min (c). All solutions were observed after 24 h.

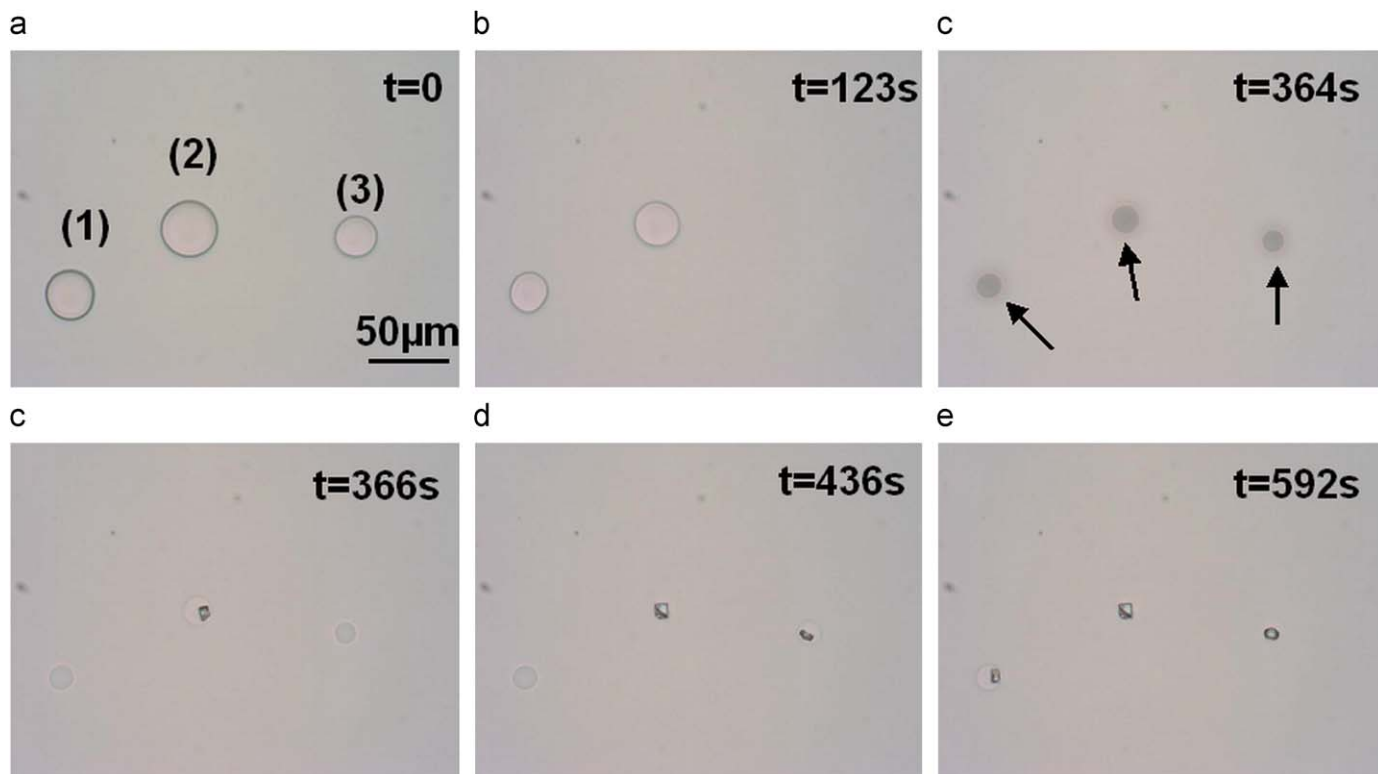


Fig. 7. Panels a–f represent time sequence showing evaporation, nucleation and growth of NaCl. (a) $t=0$:3 droplets of NaCl solutions are generated through the layer of liquid oil. In (c) the contrast was artificially enhanced.

the 0.7 M NaCl solution 1.340 is smaller than the refractive index of DMS oil 1.390. When the solution concentrates during evaporation the refractive index increases and matches the DMS oil refractive index. NaCl concentration is estimated to 6.7 M at this moment (droplet #3) in b) in the droplets from a relation between concentration and refractive index (tables 71 D-252)[59]. At $t > 140$ s droplets appear darker than the oil because they continue to concentrate (at supersaturation $\beta > 1.3$), the droplet refractive index of the NaCl solution becomes larger than the refractive index of DMS oil. Nucleation of a crystal of 10 μm occurs after 366, 436 and 592 s in droplets # (2), (3) and (1), respectively, in less than 1 s. Confinement allows stabilization of highly supersaturated solutions with respect to usual conditions, nucleation and growth occur very rapidly as in the case of precipitation, but here only one single per droplet was obtained.

5. Conclusions

Nucleation is a stochastic phenomenon and the probability of observing the critical nuclei formation is very low. In this communication we presented different unusual approaches to enhance nucleation in the metastable zone in order to locate and control it.

The first step is to determine the nucleation rate, and thus the nucleation behavior of the molecule studied. The two usual methods for determining of nucleation rate are measuring the induction time by direct counting/observation and direct determination of the steady-state rate of homogeneous nucleation.

In measuring nucleation rate, we clearly evidenced that heterogeneous nucleation affected the results. Microfluidics may offer a solution, but has limitations: evaporation through the material of the microfluidic chips, compatibility of this material with organic solvents. The second step consists in acting on nucleation, to control, locate and observe it. We studied different unusual approaches and we succeeded in enhancing nucleation in the metastable zone for external fields. Ultrasounds reduce induction time and increase the number of crystals. The light irradiation induces nucleation by forming radicals. The electric field tends to localize the nucleation near one electrode depending on the polarity of the molecule studied in acting locally on the density of the solution. Lastly confinement was tested, and results indicate that this approach is very promising for controlling spatially nucleation and moreover generate one single crystal per droplet.

These techniques, which are easy to perform at the laboratory for small quantities of products, for instance an active pharmaceutical ingredient, could be used for screening crystallization conditions and phases (polymorphism).

Acknowledgements

The authors are indebted to Sanofi-Aventis and ANR-06-Blan-0355 "MICROCRISTAL" for financial supports, for funding projects and for providing the industrial chemical compounds for the studies. We thank A.G. Bayer (Wuppertal, Germany) for providing us with BPTI, T. Bactivelane (CINaM), B. Detailleur (CINaM), M. Audiffren (Anacrismat) for technical assistance and to M. Sweetko for English revision.

References

- [1] A.C. Zettlemoyer (Ed.), *Nucleation*, Marcel Dekker, New York, 1969.
- [2] R. Boistelle, J.P. Astier, Crystallization mechanisms in solution, *J. Cryst. Growth* 90 (1988) 14–30.
- [3] D. Tsekova, S. Dimitrova, C.N. Nanev, Heterogeneous nucleation (and adhesion) of lysozyme crystals, *J. Cryst. Growth* 196 (1999) 226–233.
- [4] N.M. Dixit, A.M. Kulkarni, C.F. Zukoski, Comparison of experimental estimates and model predictions of protein crystal nucleation rates, *Colloids Surf. A Physicochem. Eng. Aspects* 190 (2001) 47–60.
- [5] D. Voss, The 110% solution, *Science* 274 (1996) 1325.
- [6] D.W. Oxtoby, Crystals in a flash, *Nature* 420 (2002) 277–278.
- [7] A. Tam, G. Moe, W. Happer, Particle formation by resonant laser light in alkali-metal vapor, *Phys. Rev. Lett.* 35 (1975) 1630–1633.
- [8] B.A. Garetz, J.E. Aber, N.L. Goddard, R.G. Young, A.S. Myerson, Nonphotochemical, polarization-dependent, laser-induced nucleation in supersaturated aqueous urea solutions, *Phys. Rev. Lett.* 77 (1996) 3475–3476.
- [9] J. Zaccaro, J. Matic, A.S. Myerson, B.A. Garetz, Nonphotochemical, laser-induced nucleation of supersaturated aqueous glycine produces unexpected polymorph, *Cryst. Growth Des.* 1 (2001) 5–8.
- [10] T. Okutsu, K. Nakamura, H. Haneda, H. Hiratsuka, Laser-induced crystal growth and morphology control of benzopinacol produced from benzophenone in ethanol/water mixed solution, *Cryst. Growth Des.* 4 (2004) 113–115.
- [11] T. Okutsu, K. Furuta, T. Terao, H. Hiratsuka, A. Yamano, N. Ferté, S. Veesler, Light-induced nucleation of hen-egg white lysozyme, *Cryst. Growth Des.* 5 (2005) 1393–1398.
- [12] S. Veesler, K. Furuta, H. Horiuchi, H. Hiratsuka, N. Ferté, T. Okutsu, Crystals from light: photochemically-induced nucleation of hen egg-white lysozyme, *Cryst. Growth Des.* 6 (2006) 1631–1635.
- [13] T. Okutsu, K. Sugiyama, K. Furuta, I. Watanebe, H. Mori, K. Obi, K. Horota, H. Horiuchi, G. Sazaki, S. Veesler, H. Hiratsuka, Photochemically induced nucleation in supersaturated and undersaturated thaumatin solutions, *J. Photochem. Photobiol. A Chem.* 190 (2007) 88–93.
- [14] D. Kashchiev, Nucleation in external electric field, *J. Cryst. Growth* 13–14 (1972) 128–130.
- [15] C.C. Chin, J.B. Dence, J.C. Warren, Crystallization of human placental estradiol 17 β -dehydrogenase. A new method for crystallizing labile enzymes, *J. Biol. Chem.* 251 (1976) 3700–3705.
- [16] M. Taleb, C. Didierjean, C. Jelsch, J.P. Mangeot, B. Capelle, A. Aubry, Crystallization of proteins under an external electric field, *J. Cryst. Growth* 200 (1999) 575–582.
- [17] M. Taleb, C. Didierjean, C. Jelsch, J.P. Mangeot, A. Aubry, Equilibrium kinetics of lysozyme crystallization under an external electric field, *J. Cryst. Growth* 232 (2001) 250–255.
- [18] C.N. Nanev, A. Penkova, Nucleation of lysozyme crystals under external electric, ultrasonic fields, *J. Cryst. Growth* 232 (2001) 285–293.
- [19] N. Mirkin, B.A. Frontana-Urbe, A. Rodriguez-Romero, A. Hernandez-Santoyo, A. Moreno, The influence of an internal electric field upon protein crystallization using the gel-acupuncture method, *Acta Crystallogr. Sect. D* 59 (2003) 1533–1538.
- [20] A. Moreno, G. Sazaki, The use of a new ad hoc growth cell with parallel electrodes for the nucleation control of lysozyme, *J. Cryst. Growth* 264 (2004) 438–444.
- [21] A. Moreno, G. Sazaki, The use of a new ad hoc growth cell with parallel electrodes for the nucleation control of lysozyme, *J. Cryst. Growth* 264 (2004) 438–444.
- [22] A. Penkova, O. Gliko, I.L. Dimitrov, F.V. Hodjaoglu, C. Nanev, P.G. Vekilov, Enhancement and suppression of protein crystal nucleation due to electrically driven convection, *J. Cryst. Growth* 275 (2005) e1527–e1532.
- [23] D.L. Worcester, Structural origins of diamagnetic anisotropy in proteins, *Proc. Natl. Acad. Sci. USA* 75 (1978) 5475–5477.
- [24] K. Lonsdale, Diamagnetic anisotropy of organic molecules, *Proc. R. Soc. London* (1939) 541–568.
- [25] D.C. Neugebauer, A.E. Blaurock, D.L. Worcester, Magnetic orientation of purple membranes demonstrated by optical measurements and neutron scattering, *FEBS Lett.* 78 (1977) 31–35.
- [26] J. Torbet, J.M. Freyssinet, G. Hudry-Clergeon, Oriented fibrin gels formed by polymerization in strong magnetic fields, *Nature* 289 (1981) 91–93.
- [27] A. Yamagishi, Biological systems in high magnetic field, *J. Magn. Mater.* 90 and 91 (1990) 43–46.
- [28] M. Ataka, E. Katoh, N.I. Wakayama, Magnetic orientation as a tool to study the initial stage of crystallization of lysozyme, *J. Cryst. Growth* 173 (1997) 592–596.
- [29] J.P. Astier, S. Veesler, R. Boistelle, Protein crystal orientation in a magnetic field, *Acta Cryst. D* 54 (1998) 703–706.
- [30] G. Sazaki, E. Yoshida, H. Komatsu, T. Nakada, S. Miyashita, K. Watanabe, Effects of a magnetic field on the nucleation and growth of protein crystals, *J. Cryst. Growth* 173 (1997) 231–234.
- [31] N.I. Wakayama, M. Ataka, H. Abe, Effect of a magnetic field gradient on the crystallization of hen lysozyme, *J. Cryst. Growth* 178 (1997) 653–656.
- [32] A. Katsuki, R. Tokunaga, S.I. Watanabe, Y. Tanimoto, The effect of high magnetic on the crystal growth of benzophenone, *Chem. Lett.* (1996) 607–608.
- [33] S.L. Hem, The effect of ultrasonic vibrations on crystallization processes, *Ultrasonics* 5 (1967) 202–207.
- [34] C. Virone, H.J.M. Kramer, G.M. Van Rosmalen, A.H. Stoop, T.W. Bakker, Primary nucleation induced by ultrasonic cavitation, *J. Cryst. Growth* 294 (2006) 9–15.
- [35] X. Chavanne, S. Balibar, F. Caupin, Acoustic crystallization and heterogeneous nucleation, *Phys. Rev. Lett.* 86 (2001) 5506LP–555509.

- [36] K. Ohsaka, E.H. Trinh, Dynamic nucleation of ice induced by a single stable cavitation bubble, *Appl. Phys. Lett.* 73 (1998) 129–131.
- [37] A. Prosperetti, Thermal effects and damping mechanisms in the forced radial oscillations of gas bubbles in liquids, *J. Acoust. Soc. Am.* 61 (1977) 17–27.
- [38] G. Ruecroft, D. Hipkiss, T. Ly, N. Maxted, P.W. Cains, Sonocrystallization: the use of ultrasound for improved industrial crystallization, *Org. Process Res. Dev.* 9 (2005) 923–932.
- [39] O. Louisnard, F.J. Gomez, R. Grossier, Segregation of a liquid mixture by a radially oscillating bubble, *J. Fluid Mech.* 577 (2007) 385–415.
- [40] R. Grossier, O. Louisnard, Y. Vargas, Mixture segregation by an inertial cavitation bubble, *Ultrasonics Sonochem.* 14 (2007) 431–437.
- [41] N. Lyczko, F. Espitalier, O. Louisnard, J. Schwartzentruber, Effect of ultrasound on the induction time and the metastable zone widths of potassium sulphate, *Chem. Eng. J.* 86 (2002) 233–241.
- [42] Z. Guo, A.G. Jones, N. Li, The effect of ultrasound on the homogeneous nucleation of BaSO₄ during reactive crystallization, *Chem. Eng. Sci.* 61 (2006) 1617–1626.
- [43] S. Ueno, R.I. Ristic, K. Higaki, K. Sato, In situ studies of ultrasound-stimulated fat crystallization using synchrotron radiation, *J. Phys. Chem. B* 107 (2003) 4927–4935.
- [44] C.N. Nanev, A. Penkova, Nucleation of lysozyme crystals under external electric, ultrasonic fields, *J. Cryst. Growth* 232 (2001) 285–293.
- [45] R. Grossier, S. Veessler, Reaching one single and stable critical cluster through finite sized systems, *Cryst. Growth Des.* 9 (2009) 1917–1922.
- [46] W. Haller, Chromatography on glass of controlled pore size, *Nature* 206 (1965) 693–696.
- [47] C.L. Jackson, G.B. McKenna, The melting behavior of organic materials confined in porous solids, *J. Chem. Phys.* 93 (1990) 9002–9011.
- [48] J.-M. Ha, J.H. Wolf, M.A. Hillmyer, W.M.D. Polymorph, Selectivity under nanoscopic confinement, *J. Am. Chem. Soc.* 126 (2004) 3382–3383.
- [49] M. Beiner, S. Rengarajan, D. Pankaj, Enke, M. Steinhart, Manipulating the crystalline state of pharmaceuticals by nanoconfinement, *Nano Lett.* 7 (2007) 1381–1385.
- [50] A.Y. Lee, I.S. Lee, S.S. Dette, J. Boerner, A.S. Myerson, Crystallization on confined engineered surfaces: a method to control crystal size and generate different polymorphs, *J. Am. Chem. Soc.* 127 (2005) 14982–14983.
- [51] J. Liu, C.E. Nicholson, S.J. Cooper, Direct measurement of critical nucleus size in confined volumes, *Langmuir* 23 (2007) 7286–7292.
- [52] R. Grossier, et al., Ultra-fast crystallization due to confinement. *J. Crystal Growth*, 2009, in press, doi:10.1016/j.jcrysgro.2009.12.020.
- [53] S. Lafont, S. Veessler, J.P. Astier, R. Boistelle, Solubility, and prenucleation of aprotinin BPTI molecules in sodium chloride solution, *J. Cryst. Growth* 143 (1994) 249–255.
- [54] T. Detoisien, M. Forite, P. Taulelle, J.L. Teston, D. Colson, J.P. Klein, and S. Veessler, A Rapid Method for Screening Crystallization Conditions and Phases of an Active Pharmaceutical Ingredient. *Organic Process Research & Development*, sous presse. (2009).
- [55] Z. Hammadi, J.P. Astier, R. Morin, S. Veessler, Protein crystallization induced by a localized voltage, *Cryst. Growth Des.* 8 (2007) 1476–1482.
- [56] Z. Hammadi, M. Gauch, R. Morin, Microelectron gun integrating a point-source cathode, *J. Vac. Sci. Technol. B Microelectron. Nanometer Struct.* 17 (1999) 1390–1394.
- [57] P. Laval, J.-B. Salmon, M. Joanicot, A microfluidic device for investigating crystal nucleation kinetics, *J. Cryst. Growth* 303 (2007) 622–628.
- [58] E. Nieto-Mendoza, B.A. Frontana-Urbe, G. Sazaki, A. Moreno, Investigations on electromigration phenomena for protein crystallization using crystal growth cells with multiple electrodes: effect of the potential control, *J. Cryst. Growth* 275 (2005) e1437–e1446.
- [59] Handbook of Chemistry and Physics, in: R.C. Weast, CRC Press, Cleveland, 1975–1976.